Cellulose Acetate Butyrate and Poly(hydroxybutyrate-co-valerate) Copolymer Blends

Charles M. Buchanan,* Steve C. Gedon, Alan W. White, and Matthew D. Wood

Eastman Chemical Company, Research Laboratories, P.O. Box 1972, Kingsport, Tennessee 37662

Received April 28, 1992; Revised Manuscript Received August 10, 1992

ABSTRACT: Blends in the composition range 20–80 wt % of cellulose acetate butyrate (CAB) and a copolymer of poly(hydroxybutyrate-*co*-valerate) (PHBV) were prepared by thermal compounding. Carbon-13 NMR and gel permeation chromatography showed that no transesterification occurred during thermal mixing and that little change in molecular weight occurred. Blends containing 20–50% PHBV were amorphous, optically clear miscible blends, while the blends containing 60–80% PHBV were semicrystalline, partially miscible blends. Both thermal and dynamic-mechanical analysis revealed the presence of a high-temperature transition that was sensitive to blend composition and a low-temperature transition whose position was largely uninfluenced by the blend composition; the high-temperature transitions of the 20–50% PHBV blends closely match calculated T_g's for a fully miscible blend. Carbon-13 NMR in the melt of the blend components and of a 50% PHBV blend revealed that even in a homogeneous melt, the CAB and PHBV have vastly different mobilities. It is proposed that the dual transitions in the blends containing 20–50% PHBV arise from dynamic heterogeneity and not from a classical miscibility gap. X-ray diffraction studies of the crystalline blends indicate that the PHBV crystallalizes in a morphology unique from the PHBV blend component. Blend morphology was found to strongly influence physical properties such as tensile strength and tangent modulus; blends containing 70% and 80% PHBV were found to exhibit tear strengths that were superior to either of the blend components.

Introduction

The concept of polymer blends and their industrial utilization is now well established in the polymer scientific community. By current theory, polymer blends are classified as miscible, partially miscible, or immiscible. Generally, miscible polymer blends are considered to be amorphous materials which are microscopically homogeneous and are characterized by features such as optical clarity and a single glass transition temperature when measured by thermal or dynamic-mechanical techniques. Partially miscible blends, although they contain a significant amount of microscopic mixing, display microscopic heterogeneity and characteristically will display two or more glass transition temperatures intermediate between those of the blend components. Barring similar indices of refraction, partially miscible blends tend to be hazy to opaque. Immiscible blends are macroscopically heterogeneous, displaying multiple glass transition temperatures, including those of the homopolymer blend components. Because of features such as optical clarity, predictable physical properties, and simplfied processing, miscible blends are often preferred. Relative to miscible blends or the blend components, partially miscible blends (often termed mechanically compatible blends) can often provide superior physical properties, but these properties can depend strongly on processing conditions. Immiscible blends generally give poor physical properties although rubber or glass modified polymer blends are notable exceptions. The boundary between these various classes of blends is often not clear, particularly in cases were compatibilitizers are employed to increase interactions between two marginally miscible homopolymers.

A number of excellent articles and reviews[1-7] have appeared which describe the fundamental factors which determine blend miscibility. The most basic requirement for polymer blend miscibility is that the free energy of mixing ($\Delta G_{mix} = \Delta H - T\Delta S$) be negative. A number of structural and morphological characteristics have been shown to directly influence polymer–polymer interactions including hydrogen-bonding interactions, blend compo nent molecular weight, crystallinity, surface energy, an dipolar interactions, as well as factors related to blen formation such as physical mixing, temperature, solven (s), or solvent(s) removal.

Cellulose esters are perhaps one of the oldest therm plastics in the chemical industry. Industrially, the mo important thermoplastic cellulose esters are cellulo acetates (CA), cellulose acetate propionates (CAP), an cellulose acetate butyrates (CAB) with a degree of sul stitution (DS) in the range 2.5–3.0. These cellulose este typically have melting temperatures in the 150–250 ° range. Those cellulose esters which have a combinatic of high melt temperature and high melt viscosity ofte will discolor and suffer loss of physical properties due t thermal decomposition during melt processing. Cons quently, monomeric plasticizers such as dialkyl phthalat or triaryl phosphates are added to lower melt processir temperatures. These plasticizers also serve a dual functic in that they are used to modify other parameters such a the flexural strength, tensile strength, flexural modulu or impact strength of the molded object. Although the plasticizers serve a vital role, they in fact cast limitatio on cellulose ester thermoplastics because of their lo molecular weight. Plasticizers can lower melt strengt and will often volatilize during melt processing of th cellulose ester. Plasticizer also tends to narrow the ran of achievable physical properties and can migrate fro the finished product.

Some time ago, we initiated a program to investiga cellulose ester/polymer blends. Our goals have bee multiple. We have sought primarily to find optically cle thermally processable blends with useful physical pro erties and to understand the relationship between ble morphology and physical properties. We have also bee interested in partially miscible blends which have e hanced physical properties relative to those of the ble components. In addition to using these types of blen in classical thermoplastic applications, we are intrigue

by the potential of using cellulose ester/polymer blends as biodegradable polymers.[8] Surprisingly, blends of cellulose esters with other natural of synthetic polymers have generally received very little attention. Most notable among the sparse accounts available is the work by Koleske et al.,[9] who reported that solvent cast blends of cellulose esters and polycaprolactone were miscible. Later by Hubbell and Cooper[10] indicated that CAB/polycaprolactone blends were partially miscible. Very recently, Scandola et al. have disclosed that polyhyroxybutyrate (PHB) forms miscible blends with cellulose esters.[11] Prompted in part by the work of Scandola,[12] we would like to share our findings concerning blends of a CAB (DS = 2.6; DS_{Bu} = 1.6, DS_{Ac} = 1.0, structure 1) with poly(hydroxybutyrate-*co*-valerate) (PHBV, structure 2) [90/10].

Structure 1 Cellulose acetate butyrate

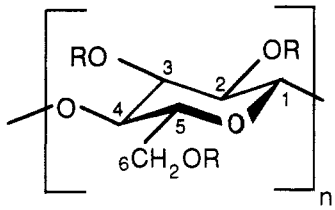

R = butyryl, acetyl, or hydrogen

Structure 2 Poly(hydroxybutyrate-co-valerate)

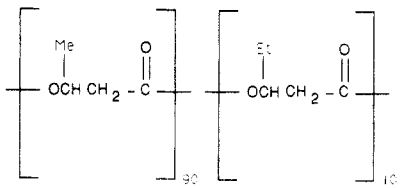

Experimental Section

CAB (CAB 381-20) was obtained from Eastman Chemical Co., and PHBV was obtained from ICI. These polymers were used without further purification. Debris, assumed to be cellular material, was evident in the PHBV.

The blends were prepared by first mixing the blend components in a plastic bag before compounding at 185 °C in a Rheometrics mechanical spectrometer for 5 min.[13] The resulting blend was ground to 5-mm particle size, and a portion was pressed between two metal plates at 180 °C and then allowed to cool slowly at ambient temperature to form a film which was typically 4–5 mm thick. The tensile strengths, elongations at break, and tangent modulii of the films were measured by ASTM Method D882; the tear strength was measured by ASTM Method D1938.

Inherent viscosities were measured at a temperature of 25 °C for a 0.5-g sample in 100 mL of a 60/40 by weight solution of phenol/tetrachloroethane.

GPC data were acquired on a Waters Model 150C gel permeation chromatograph. The mobile phase was $CHCl_3$, and the sample size was 20–25 mg/10mL. The molecular weights are reported in polystyrene equivalents.

Solution-state carbon-13 NMR spectra were collected on JEOL Model GX 270-MHz spectrometer operating at 67.8 MHz. The spectra were collected at ambient temperature with a sample concentration of 100 mg/mL $CDCl_3$. The center peak of $CDCl_3$ was used as an internal reference which was taken to be 77.0 ppm. Carbon-13 NMR spectra in the bulk melt were collected on a JEOL Model GX-400 MHz spectrometer operating at 100 MHz using a Doty high-temperature 10-mm solution-state probe. Samples were prepared by consecutively placing small portions of the sample in a 5-mm tube which was then placed in a heat block heated to 185 °C for PHBV and the 1/1 CAB/PHBV blend and 235 °C for CAB. Air was forced from the melted sample by insertion of a stainless steel metal bar. The 5-mm tube was then inserted into a 10-mm tube containing molten biphenyl-d_{10} which served as an internal lock. The 5-mm tube was held in place by Teflon O-rings at the top and bottom of the 10-mm tube. The spectra were collected on nonspinning samples using a pulse delay of 10 s. Typically, 1K–4K scans were used to collect each spectrum. All NMR spectra were processed by using a 8-Mbyte Mac II Macintosh Computer, with VersaTerm Pro as an emulation package and MacDraw II as a graphics package, interacting with Hare's FTNMR software running on a VAX 8800 computer.

The IR spectra were collected on a Nicolet 5DX spectrometer using melted samples.

Dynamic mechanical thermal analysis was accomplished using a Polymer Laboratories Mk II spectrometer operating at 4 °C/min and 1 Hz. Samples were melt-pressed films cooled slowly from the melt at ambient temperature which were prepared using metal plates having a preformed well of 20 mm.

The DSC spectra were collected using a Du Pont 912 differential scanning calorimeter spectrometer. At least two individual measurements were made to ensure reproducibility. Each sample was heated from −20 to +200 °C at a heating rate of 20 deg/min before cooling at 20 deg/min to −20 °C. Second scan heating curves were then collected by heating from −20 to +200 °C. All T_g's were taken from the second scan and are reported as T_g onset and T_g midpoint. The T_g onset was determined by measuring the intercept formed by extrapolation of the baseline proceeding the transition and the tangent of the transition. The T_g midpoint was taken to be the midpoint of the tangent between the intercepts formed by extrapolation of the baseline preceding and following the transition and the tangent of the transition.

Wide-angle X-ray diffraction experiments were preformed using a Scintag PAD V X-ray diffractometer using Cu Kα X-rays with a voltage of 45 kV and a current of 20 mA and a pressed graphite diffracted beam monochromator. Crystallinities were determined by fitting Gaussian peaks to each of the crystalline peaks; a single Gaussian peak was used to approximate the amorphous curve. The percent crystallinity was calculated using the equation, % C = $\sum A_c/\sum A_c + \sum A_a$, where A is the area of the absorption band, a is the amorphous band, and c is the crystalline band.

Scanning electron micrographs (SEM) were obtained on a Cambridge Instruments Stereoscan 200 scanning electron microscope. All specimens were submerged into liquid N_2, fractured, and then sputter coated with a thin layer of gold (<200 Å) before SEM observations.

Results and Discussion

Bacterial polyhydroxybutyrate (PHB) is isotatic and is both highly crystalline and sensitive to heat (decomposition temperature ca. 170–190 °C).[13] Consequently, fermentation conditions and bacterial strains are often selected which promote the incorporation of hydroxyvalerate into the PHB, resulting in a copolymer with lower crystallinity and a lower melt processing temperature. Selection of the blend components of this study were also dictated by many of the same considerations. The PHBV was selected on the basis that it would offer a relatively good melt processing window (ca. 170–185 °C). The cellulose acetate butyrate (CAB) was chosen because of its match in molecular weight (Table I) with the PHBV and because of its high acetyl/butyrl ratio (1.0/1.6). The acetyl/butyryl ratio provides for a relatively low T_m (165 °C) and high T_g (125 °C). The low T_m of the CAB is of course vital, but in many respects the T_g is of equal importance. In miscible, amorphous blends where the T_g of the blend changes linearly as a function of the weight percent of blend components, a blend component with a high T_g extends the composition range of a blend where the T_g of the blend is maintained above room temperature.

The blends of this study were prepared by thermally compounding only. Although some loss in molecular weight is observed, the number average molecular weights of the blends are maintained in the 43 000–73 000 range

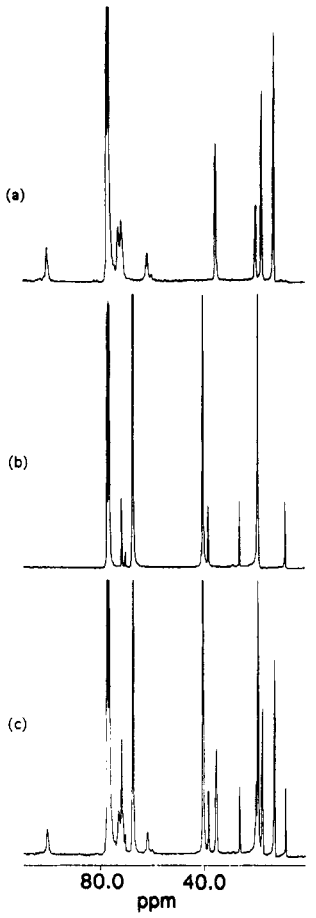

Figure 1. Solution-state carbon-13 NMR spectra of (a) the aliphatic carbons of CAB, (b) the aliphatic carbons of PHBV, and (c) the aliphatic carbons of a 1/1 CAB/PHBV blend.

Table I
Molecular Weights of CAB, PHBV, and CAB/PHBV Blends As Measured by GPC

blend CAB/PHBV	10^4M_n	10^5M_w	10^5M_z	M_w/M_n	M_z/M_n
100/0	5.66	1.39	2.90	2.45	5.12
80/20	5.14	1.35	3.10	2.63	6.03
70/30	5.09	1.39	3.04	2.73	5.97
60/40	5.14	1.44	3.24	2.81	6.31
50/50	4.29	1.42	3.34	3.31	7.81
40/60	5.39	1.53	3.39	2.84	6.29
30/70	6.57	1.66	3.92	2.53	5.97
20/80	7.32	1.57	3.32	2.15	4.53
0/100	8.84	1.90	3.94	2.15	4.46

(Table I). Esterification or transesterification of the CAB with the PHBV potentially could occur in melt processing of these blends. With regard to the GPC measurements in Table I, the relatively tight band of M_z values does not indicate large increases in molecular weght. To probe the question of transesterification further, we examined the blends in detail using solution-state carbon-13 NMR spectroscopy. Figure 1a shows the resonances of the ring carbons of the CAB,[14] Figure 1b gives the non-carbonyl carbon resonances of the PHBV, and Figure 1c is the carbon-13 NMR spectrum of a 50/50 blend of the two components. In Figure 1a, the C1 ring carbon resonance adjacent to a substituted C2 is centered at 100 ppm while the downfield resonance at 102 ppm is due to a C1 carbon adjacent to a C2 which does not bear an acyl substitutent. Similarly, the carbon resonance at 62 ppm is due to a substituted C6 carbon and the resonance at 60 ppm results from a unsubstituted C6 carbon. Comparison of Figure 1a,c shows that these resonances remain unchanged in the

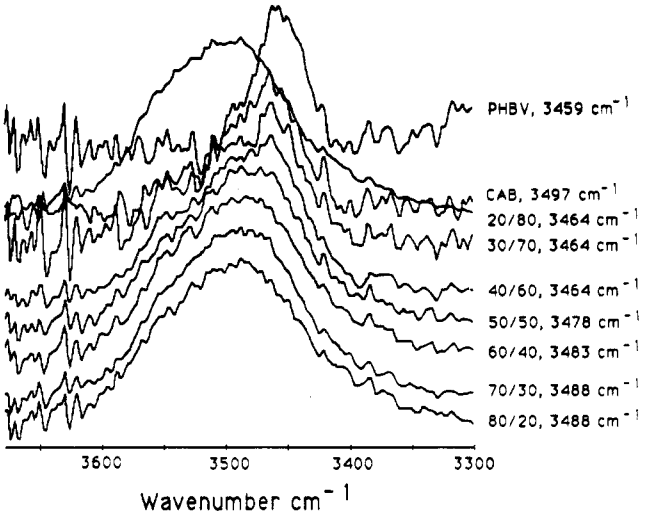

Figure 2. The O–H stretching region in the IR spectra of CAB and CAB/PHBV blends. The compositions as well as the peak maximums are indicated. The bands have been scaled to the same percent transmittance.

blend, indicating that the degree of substitution of the CAB has not changed from the blending operation. Furthermore, no new resonances appear in the spectrum of the blend. The ^{13}C NMR carbonyl spectral region (not shown) of these same blends also showed no new peaks which could be attributed to transesterification.

In order to gain insight with regard to blend structure and miscibility, we examined each blend using infrared spectroscopy. The carbonyl and the fingerprint regions were heavily overlapped but useful information could be obtained from the O–H stretching region from 3700 to 3300 cm^{-1}. Figure 2 gives the IR spectra for the 20–80% PHBV blends as well as for the two blend components. (The bands have been scaled to 100% transmittance and are not indicative of relative OH content.) The CAB absorption band, which is very broad, is centered at 3497 cm^{-1} and is indicative of intramolecular hydrogen bonding of hydroxyls.[15] The weak PHBV absorption band, presumably due to hydroxyl end groups, gives a somewhat sharper but still broad band centered at 3459 cm^{-1}, which is again consistent with intramolecular hydrogen bonding. Although the broadness of the bands does not provide for good resolution, it is apparent that for the 20–50% PHBV blends, the O–H stretching bands remains broad and symmetrical while shifting to lower frequencies intermediate between that of pure PHBV and CAB with increasing PHBV content in the blend. Above 60% PHBV in the blend, the O–H stretching absorption band becomes dissymmetrical and remains fixed at 3464 cm^{-1}. The observation of broad bands with small OH frequency shifts in the region 3460–3500 cm^{-1} that do not depend linearly upon blend composition is not consistent with blend compatibilization due to hydrogen bonding.

As noted in the Experimental Section, no effort was made to remove any remaining cell wall debris which imparted a haze to all of the blends. Nevertheless, it was very evident that the blends containing 20–50% PHBV were clear while those with greater than 50% PHBV were opaque. Parts a, and b, of Figure 3 are SEM photographs of the 80/20 and 20/80 blends, respectively. These photographs show that the 80/20 blend has a very smooth texture with no evidence of phase separation. The 20/80 blend texture has a more mottled appearance but no distinct phase boundaries were observed. If distinct phases are present in these blends, domain sizes must be less than 300 Å.

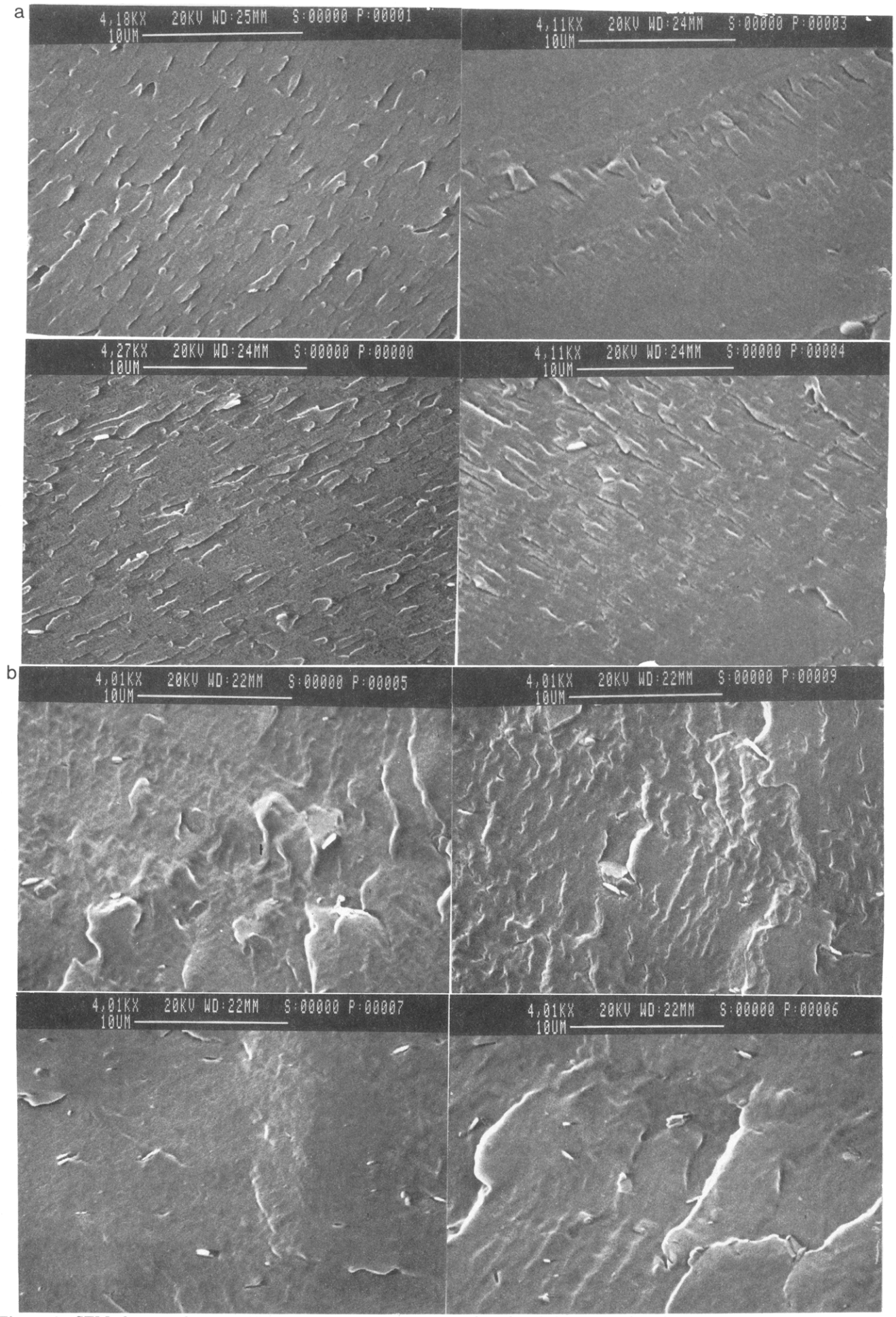

Figure 3. SEM photographs (magnification = 3000) of (a) an 80/20 blend and (b) a 20/80 blend.

Table II
Experimental DSC T_m's and T_g's, Experimental DMTA T_g's, and Calculated DSC and DMTA T_g Values for CAB and PHBV Blends

blend CAB/PHBV	T_m[a] (°C) first cycle	T_m (°C) second cycle	T_{ch} (°C) second cycle	T_g[b] (°C) DSC	T_g[c] (°C) DMTA	T_g[d] calc (°C) DSC	T_g[d] calc (°C) DMTA
100/0	169 ΔH_f = 3.3	ND	ND	129 (121)	160		
80/20	ND	ND	ND	11, 100 (10, 98)	40, 135	104 (96)	136
70/30	ND	ND	ND	13, 78 (7, 67)	45, 122	91 (83)	125
60/40	ND	ND	ND	9, 69 (6, 56)	45, 115	78 (70)	113
50/50	ND	ND	ND	8, 66 (4, 54)	45, 105	66 (58)	101
40/60	159 ΔH_f = 9.4	154, 163	ND	8, 60 (4, 51)	44, 77	53 (45)	89
30/70	159 ΔH_f = 11.4	155, 163	102	7, 53 (3, 47)	46	40 (32)	77
20/80	160 ΔH_f = 13.7	156, 164	93	5, 44 (1, 34)	46	27 (19)	66
0/100	166 ΔH_f = 19.0	157, 167	ND	−2 (−6)	42		

[a] The heats of fussion are taken from the first cycle and are reported in cal/g. [b] The T_g values are taken from the second scan. The values are the T_g midpoints, while the values in parentheses are the T_g onsets. [c] The tan δ's for the high-temperature transition of the 30/70 and 20/80 blends were very broad and are not reported. [d] These values were calculated using the equation $T_{g12} = T_{g1}W_1 + T_{g2}W_2$, where T_{g12} is the T_g of the blend, T_{g1} and T_{g2} are the T_g's of the blend components, and W_1 and W_2 are the weight fractions of the components in the blend.

To probe the question of blend miscibility, DSC and DMTA spectra were collected for the blends and the blend components; the analysis of these spectra have been summarized in Table II along with calculated T_g values. Parts a and b of Figure 4 show the storage modulus, E' and mechanical loss tangent, tan δ, respectively, for the blend components and each of the blends as measured by DMTA. Looking first at E', the CAB shows a single sharp transition at 160 °C with no evidence of a low-temperature relaxation process. The blends containing 20–50% PHBV show two relaxation processes, a low-temperature transition centered near 45 °C and another high-temperature transition. The high-temperature transitions, which are clearly associated with the glass transition temperatures of the blends, decrease linearly while the low-temperature transitions are relatively constant and presumably associated with that of PHBV. At 60% PHBV, the storage modulus initially falls only to rise again which we interpret to be due to crystallization once the temperature has been raised above that of the T_g of the blend. In contrast, E' of the blends containing 70% and 80% PHBV are virtually superimposable and are very similar to that of the PHBV. The tan δ curves shown in Figure 4b (some were omitted for clarity) follow very much the same pattern as those of E'. Of particular interest is tan δ for the 40/60 blend in which both the high- and low-temperature transitions are very pronounced. In analogy with the DMTA spectra, the DSC spectra showed both a low- and high-temperature relaxation (Table II). In moving from 20% to 80% PHBV, the low-temperature relaxation onset shifted from 10 to 1 °C and became more pronounced while the high-temperature transitions were very broad. Table II also shows that in the range 20–50% PHBV, T_g's measured by DMTA closely agree with calculated values while the T_g's measured by DSC show a negative deviation from theoretical. Above 50% PHBV, the blend T_g's (DSC) begin to show a positive deviation from calculated values.

Figure 5 shows first and second scan DSC heating curves for the blends containing 50–80% PHBV. In the first scan, the blend containing 50% PHBV (as well as the 20%, 30%, and 40% PHBV blends which are not shown) does not show a melting peak while the 60, 70, and 80% blends show broad, ill-defined melting peaks. As shown in Table II, ΔH_f from the first scan heating curves increase linearly with increasing percent PHBV, intercepting the value for pure PHBV. The second scan DSC heating curves show similar melting peaks with smaller values for

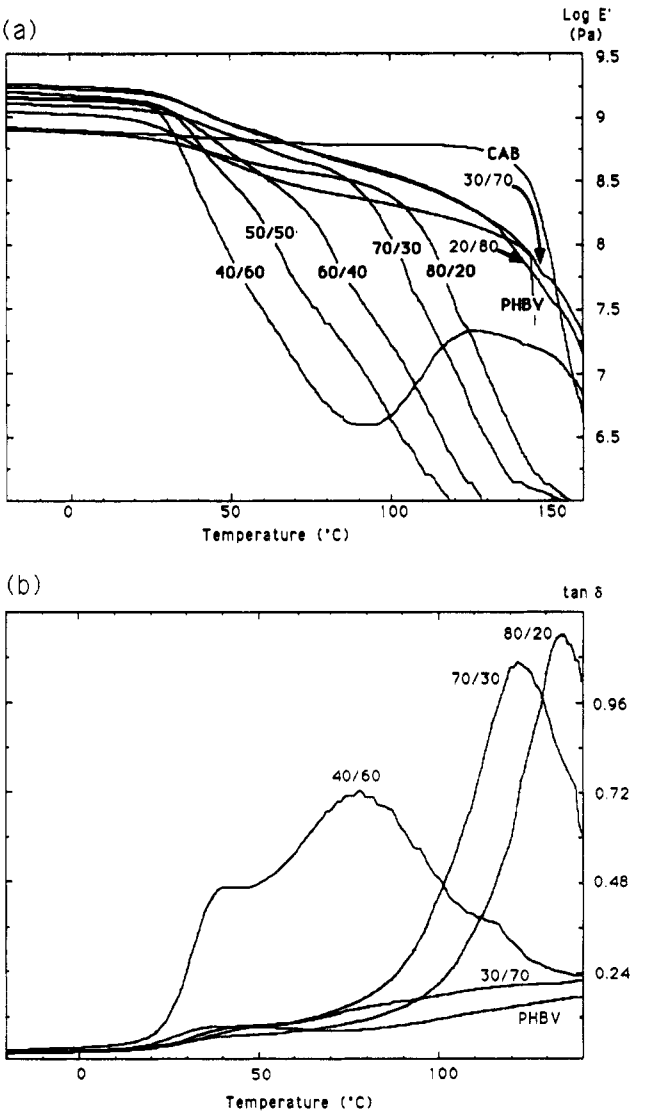

Figure 4. (a) Storage modulus, E', and (b) loss tangent, tan δ, measured for CAB, PHBV, and CAB/PHBV blends. Some of the tan δ curves were omitted for clarity.

ΔH_f relative to the first scan. Crystallization on heating (T_{ch}), characterstic of PHBV copolyesters containing 10% valerate quenched from the melt,[16] was supressed until the PHBV content of the blends reached 70%; crystal-

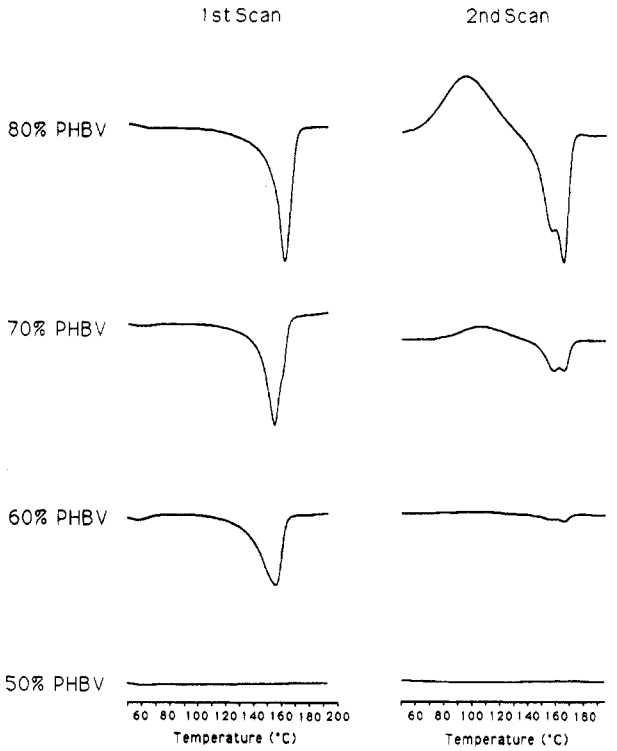

Figure 5. First and second scan heating curves for CAB/PHBV blends.

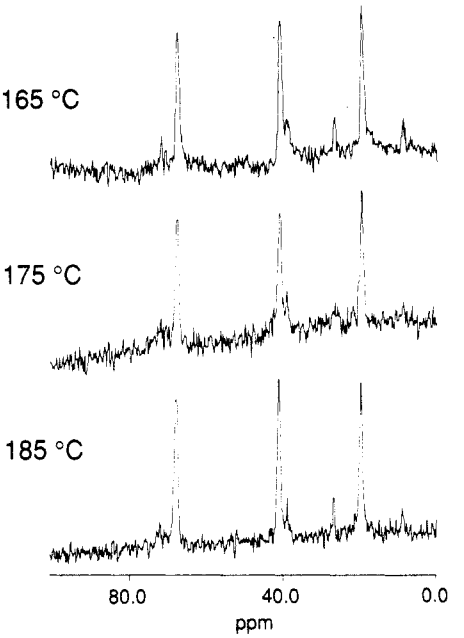

Figure 6. Carbon-13 NMR spectra of PHBV at 165, 175, and 185 °C (bulk melt).

lization during cooling (20 deg/min) for these blends was not observed.

Earlier we noted that nearly all accounts which describe miscible polymer blends generally require the presence of a single glass transition temperature when measured by thermal or dynamic-mechanical techniques. Two or more glass transition temperatures intermediate between those of the blend components or a single broad T_g are characteristic of blend heterogeneity. Ignoring, for the moment, the presence of the relatively fixed, low-temperature relaxations in the DSC and DMTA spectra, we find that in the range 20–50% PHBV the T_g decreases linearly according to the the Fox–Flory equation. As we have noted, these same blends are amorphous, optically clear, and show no evidence of phase separation by SEM. In short, they meet most criteria for a miscible blend except for the low-temperature T_g. The classical, but unsatisfying, explanation for these observations is that the blends are actually partially miscible blends consisting of a miscible CAB/PHBV phase and a PHBV phase where the ratio of the mixed phase to the PHBV phase is very large and the domain size of the two phases are small.

The basis for a single T_g in polymer blends, as measured by thermal or dynamic-mechanical techniques, is the expectation that for homogeneously mixed systems, all components will experience equivalent or average free volumes.[17] However, equivalent free volumes does not necessarily imply a single glass transition temperature. Scandola, et al.[18] have shown that for polymer–diluent mixtures, dual mobilization of two components in a otherwise homogeneous mixture may in fact be common. Miller et al.[19] have demonstrated that broad glass transition temperatures do not necessarily imply morphological heterogeneity. Rather, a broad T_g can reflect differing molecular motions of the blend components. The components of the blends described in this work have widely separated T_g's and much different molecular mobilities. It is well-known that both in solution and in the solid state cellulose esters are rigid extended helices or ribbons while nonaromatic polyesters or polyolefins are generally random coils with good molecular mobility.[20] Our current belief is that the amorphous blends are indeed morphologically homogeneous and that the dual transitions result not from nonequivalent free volumes but rather from nonequivalent molecular motions of components with equivalent free volumes.

To probe this question further we examined CAB, PHBV, and a 50% PHBV blend in the melt by carbon-13 NMR. What is immediately evident from these spectra (Figures 6 and 7) are the differences in the mobility of the carbons in the melt for the two polymers individually and in the blend (for clarity of presentation, we do not show the carbonyl carbons). At 165 °C, all of the PHBV carbon resonances are relatively narrow, indicating liquidlike mobility (Figure 6). The line width of the PHBV carbon resonances are largely unaffected as the temperature is increased to 185 °C (due to the thermal instability of the PHBV, we are limited to 185 °C). In contrast, the CAB ring carbon resonances as well as those of the methyl and methylene carbon resonances of the butyryl and acetyl substituents are lost in the baseline at 185 °C, a characteristic typical of solidlike mobility (Figure 7). At 235 °C (70 deg above the melting temperature), the resonances for the methyl and methylene carbon resonances of the butyryl and acetyl substitutents are observed while the ring carbon resonances are still spread in the baseline, demonstrating that solid and liquid type mobility can coexist in the CAB. The spectrum for the 50% PHBV blend (185 °C) shows that the line widths of the PHBV carbon resonances have been considerably broadened and that the CAB butyryl methyl carbon resonance is now present. Although the CAB methyl resonance is small, the line width is more narrow. The broadened line width of the PHBV resonances indicate that the PHBV has decreased mobility, and the appearance of the CAB resonance suggests that the polysaccharide side chain has increased mobility. However, even in a homogeneous melt, the blend components have much different mobilities. We believe that this difference in molecular mobility or dynamic heterogeneity is maintained in the solid and that it is reflected in thermal or dynamic analysis as two T_g's, a high-temperature transition characteristic of a fully miscible blend and a low-temperature β transition asso-

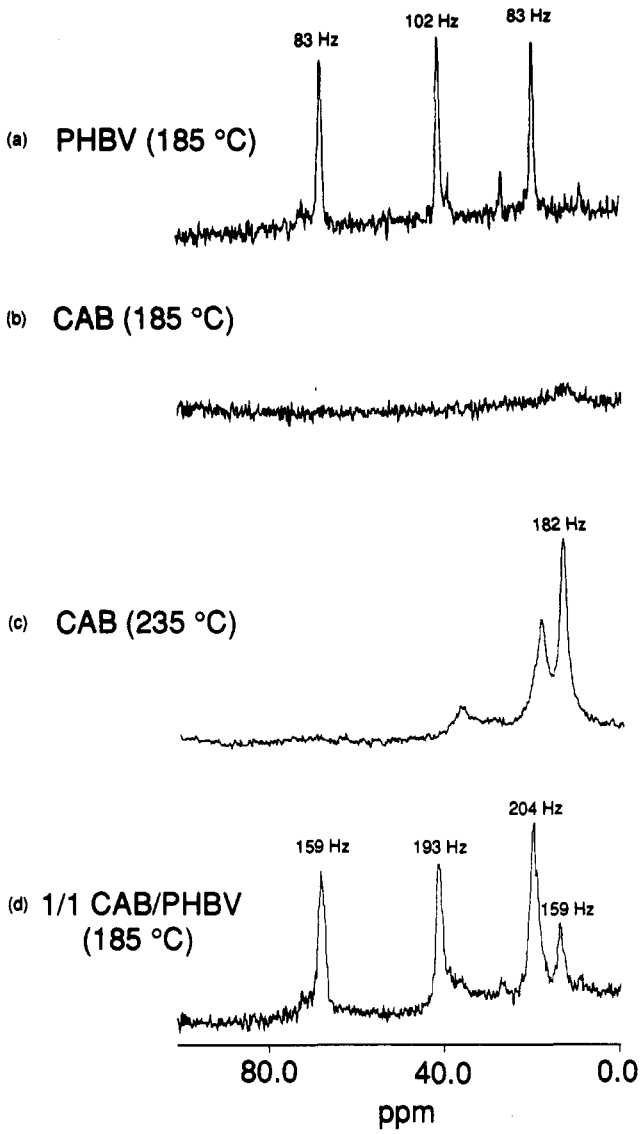

Figure 7. Carbon-13 NMR spectra in the melt of (a) PHBV at 185 °C, (b) CAB at 185 °C, (c) CAB at 235 °C, and (d) a 1/1 blend of CAB/PHBV. Tbe line widths (in Hz) of the PHBV resonances at 0.5 peak height are given for each peak.

ciated with that of PHBV whose position is relatively unaffected by blend composition.[21]

We were quite intrigued with the crystallization of the blends containing high levels of PHBV and, consequently, examined each of the blends by wide-angle X-ray diffraction (WAXD). Consistent with DSC, the 20–50% blends were amorphous and very much resembled the CAB while the 60–80% blends exhibited increasing crystallinity (Figure 8). Although the WAXD patterns for the 70% and 80% PHBV blends resembled pure PHBV in many respects, the band at $2\theta = 20°$ is noticeably absent and the bands at $2\theta = 13.7$ and 17.2° are much more narrow and intense relative to the PHBV (Figure 9). Rather that just simple suppression of the total crystallinity of the PHBV in the blend, WAXD indicates a different crystalline morphology. A different crystalline morophology is also indicated by the crystallinity index (CI, Table III), determined from the ratio of the total crystallinity of a blend to that of PHBV which is taken to be 100% crystalline (an aribary assumption). The blend containing 80% PHBV has a CI of 102%; if the CI is corrected to include the weight percent of PHBV in the blend, the blend with 80% PHBV has a CI of 128%. Furthermore, we also found that the bands at $2\theta = 13.7$ and 17.2° for the 80% PHBV blend have a larger crystallite size than

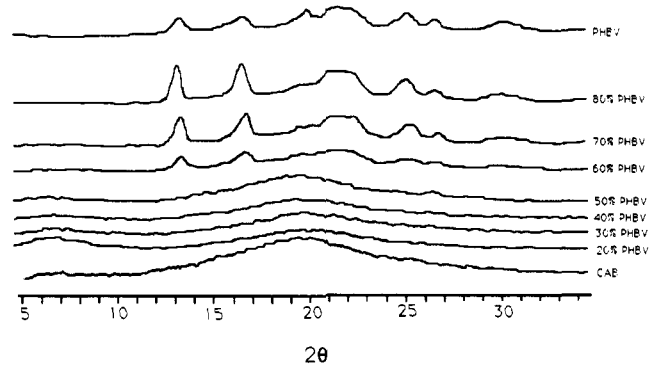

Figure 8. Wide-angle X-ray diffraction patterns for CAB, PHBV, and 20–80% PHBV blends.

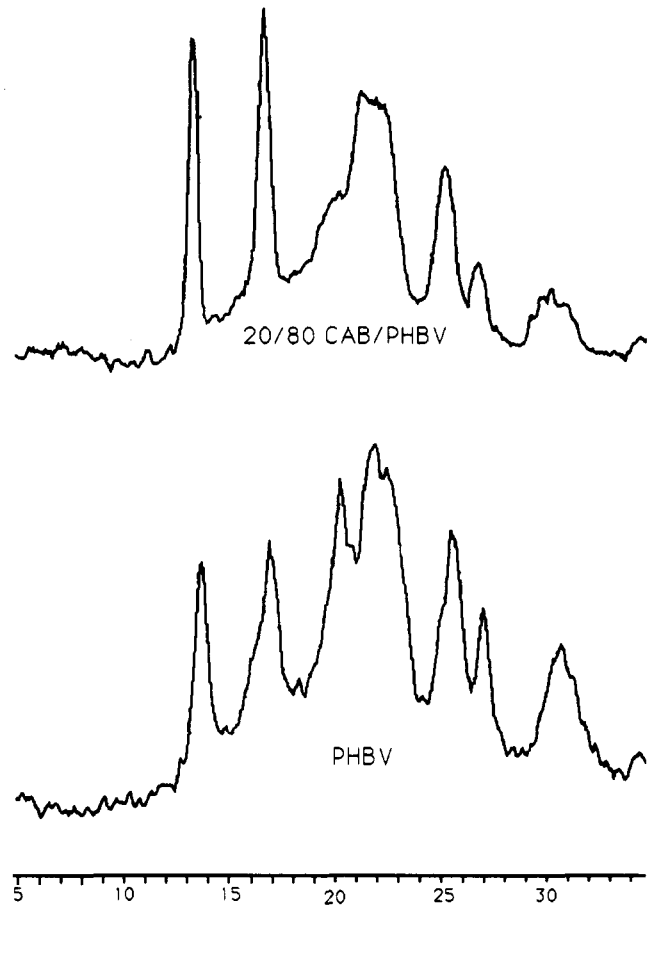

Figure 9. Wide-angle X-ray diffraction patterns for the blend containing 80% PHBV and PHBV.

Table III
Crystallinity Index and Crystallite Size from Wide-Angle X-ray Analysis

blend CAB/PHBV	CI (%)	CI/W_f PHBV (%)	crystallite size (Å) 13.7°	17.2°
40/60	56	93	104	95
30/70	86	123	138	116
20/80	102	128	170	137
0/100	100	100	113	89

that of PHBV. The basis for this observation is not clear from our data and warrents further study.

Mechanical Properties

Of particular interest to us is the relationship between blend morphology and physical properties. From expe-

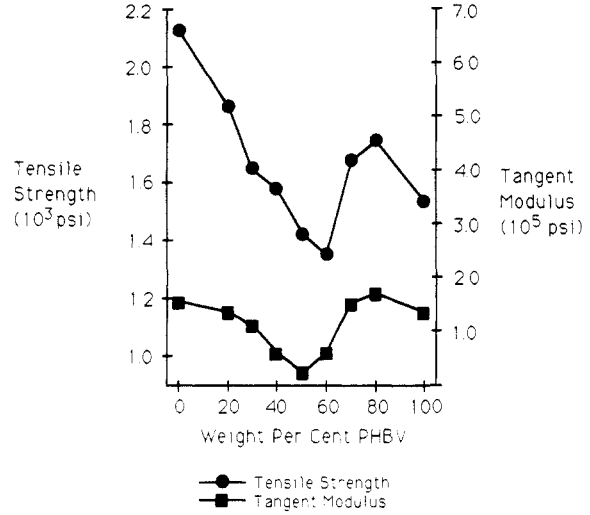

Figure 10. Change in tangent modulus and tensile strength of the CAB/PHBV blends containing 0–100% PHBV.

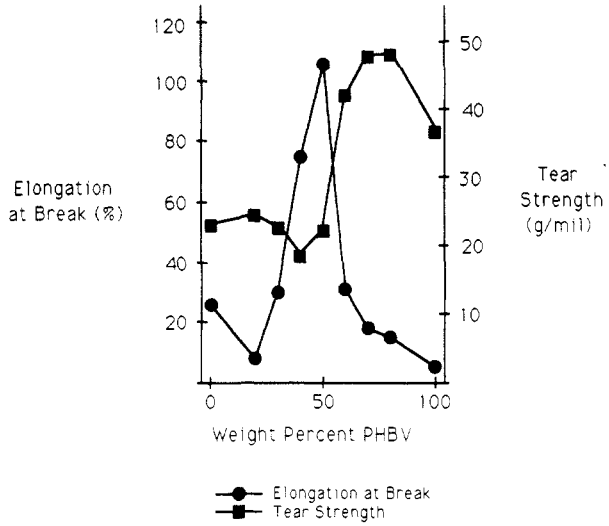

Figure 11. Change in tear strength and elongation at break of the CAB/PHBV blends containing 0–100% PHBV.

rience, we have found melt-pressed films to be a convenient and rapid means for evaluation of the physical properties or polymer blends. Figures 10 and 11 give the parameters we typically monitor and illustrate their values for the blends of this study as well as for the blend components. The properties of the CAB are typical of most nonplastized cellulose ester thermoplastics; cellulose ester films generally have high tensile strengths and modulii as well as low elongations at break and tear strengths. The physical properties shown for PHBV reflect the high crystallinity of the polymer; the PHBV films have virtually no elongation at break, and the tangent modulus is relatively high for a material with relatively low tensile strength. As is shown in Figures 10 and 11, in the range 20–50% PHBV, the tangent modulii and tensile strengths decrease in a linear fashion. The tear strengths are largely unaffected while, quite remarkably, the elongation at break increases to 106%. These changes in physical properties, of course, reflect the amorphous character of the blends containing 20–50% PHBV. Above 50% PHBV where the crystallinity of the PHBV is no longer suppressed, the tangent modulii, the tensile strengths, and the tear strengths increase with increasing PHBV in the blends while the elongations at break drop significantly. Of particular interest is the observation that at 70% and 80% PHBV in the blend, the values of all of the parameters are raised relative to 100% PHBV. While one could possibly explain the changes in the tensile strength, tangent modulus, and elongation at break on the basis of additivity, the improvement of the tear strength to a value larger than both blend components cannot. As we have noted above, we believe that the 70% and 80% blends have a much different crystalline morphology relative to 100% PHBV. We believe that this difference is largely responsible for the observed physical properties of these blends.

Conclusion

For both scientific and commercial reasons, polymer blends which give physical properties that are enhanced and/or unique from the blend components are extremely attractive. Because of their high crystallinity and instability to heat, commercial uses of isotatic PHB and copolymers of PHB have been limited. High production costs and limited availability have also limited the commercial exploitation of PHB. In this context, we have shown that by thermally mixing PHB with a polysaccharide, a blend with unique and useful physical properties can be obtained. The cellulose ester also lowers the volume of PHB needed to manufacture a given object. As we have shown, by proper choice of the ratio of blend components, either an amorphous or a semicrystalline material is obtained whose physical properties are unique and are not the result of additivity. We expect that these blends will find commercial utility, particularly in the area of biodegradable thermoplastic polymers.

We also find the question of blend miscibility and morphology for these materials to be intriguing. The blends which contain 60–80% PHBV are clearly partially miscible blends whose morphology is driven by crystallization of the PHBV. For the amorphous blends, optical microscopy indicates domains less than 300 Å while IR spectroscopy does not reveal any specific interactions between the blend components. Thermal and dynamic mechanical analysis reveals two relaxation transitions, a high-temperature transition whose value matches closely that calculated for a fully mixed and miscible system and a low-temperature relaxation associated with that of the PHBV. Carbon-13 NMR spectra obtained for the 50% PHBV blend indicate dynamic heterogeneity in the melt. We propose that the 20–50% PHBV blends are in fact miscible and that the dual transitions observed by DSC and DMTA are due to dynamic heterogeneity. Additional work is certainly warranted; this work is in progress and will be reported in due course.

Acknowledgment. The authors are grateful to Eastman Chemical Co. for supporting this work. The contributions of Eddie Forbes, Rick McGill, Gene Wooten, and Dr. Doug Lowman to this work have been particularly valuable.

References and Notes

(1) Barlow, J. W.; Paul, D. R. *Polymer* **1984**, *25*, 487.
(2) Brannock, G. R.; Paul, D. R. *Macromolecules* **1990**, *23*, 5240.
(3) Qin, C.; Pires, A. T. N.; Belfiore, L. A. *Macromolecules* **1991**, *24*, 666.
(4) Parmer, J. F.; Dickinson, L. C.; Chien, J. C. W.; Porter, R. S. *Macromolecules* **1989**, *22*, 1078.
(5) Clark, M. B., Jr.; Burkhardt, C. A.; Gardella, J. A. *Macromolecules* **1991**, *24*, 799.
(6) Linder, M.; Henrichs, P. M.; Hewitt, J. M.; Massa, D. J. *J. Chem. Phys.* **1985**, *82*, 1585.
(7) Lu, X.; Weiss, R. A. *Macromolecules* **1991**, *24*, 4381.
(8) Buchanan, C. M.; Gardner, R. M.; Kromarck, R. G. Aerobic Biodegradation of Cellulose Acetate. Cellulose 91, New Orleans, LA, December 1991.
(9) Koleski, J. V.; Whitworth, C. J.; Lundberg, R. D. U.S. Pa. 3,-922,239, 1975.

(10) Hubbell, D. S.; Cooper, S. L. *J. Appl. Polym. Sci.* **1977**, *21*, 3035.
(11) Scandola, M.; Ceccorulli, G.; Pizzoli, M. Blends of Cellulose Esters with Bacterial Poly(3-hydroxybutyrate. Cellulose 91, New Orleans, LA, December 1991.
(12) Scandola, M.; Ceccorulli, G.; Pizzoli, M. Miscibility of Bacterial Poly(3-hydroxybutyrate) with Cellulose Esters. To be published. Dr. Scandola very graciously exchanged data with these authors prior to submission of the manuscripts. These authors are grateful for the kind and helpful comments of Dr. Scandola.
(13) Kunioka, M.; Doi, Y. *Macromolecules* **1990**, *23*, 1933.
(14) Buchanan, C. M.; Edgar, K.; Hyatt, J. A.; Wilson, A. K. *Macromolecules* **1991**, *24*.
(15) Bellamy, L. J. *The Infra-red Spectra of Complex Molecules*; John Wiley & Sons, Inc., NY, 1954; pp 83–98.
(16) Scandola, M.; Ceccorulli, G.; Doi, Y. *Int. J. Biol. Macromol.* **1990**, *12*, 112.
(17) Wunderlich, B. *The Basis of Thermal Analysis*; Turi, E. A., Ed.; Academic Press, Inc.: New York, 1981; pp 92–234.
(18) (a) Ceccorulli, G.; Pizzoli, M.; Scandola, M. *Polymer* **1987**, *28*, 2081. (b) Scandola, M.; Ceccorulli, G.; Pizzoli, M. *Polymer* **1987**, *28*, 2081.
(19) Miller, J. B.; McGrath, K. J.; Roland, C. M.; Trask, C. A.; Garroway, A. N. *Macromolecules* **1990**, *23*, 4543.
(20) (a) Buchanan, C. M.; Hyatt, J. A.; Lowman, D. W. *J. Am. Chem. Soc.* **1989**. (b) Bovey, F. A. *Polymer Conformation and Configuration*; Academic Press, Inc.: New York, 1969.
(21) Additional evidence for dynamic heterogeneity was obtained from ^{1}H 2D NOESY experiments (Mirau, P. A.; Tanaka, H.; Bovey, F. A. *Macromolecules* **1988**, *21*, 2929). In these experiments, the blend components were observed to have different correlation times through a wide range of concentrations and mixing times. A full account of our ^{1}H 2D NMR solution-phase and ^{13}C NMR melt-phase work will be presented elsewhere.

Registry No. CAB, 9004-36-8; PHBV, 80181-31-3.